



Finite element modeling of Guastavino tiled arches

E. P. Saliklis, S. J. Kurtz & S. V. Furnbach
*Dept. of Civil and Environmental Engineering,
Lafayette College, USA*

Abstract

An investigation of Rafael Guastavino's arches has been conducted by means of finite element modeling and laboratory experimentation. A novel method of modeling laminated masonry tile construction via the finite element method has been devised. This technique takes advantage of the layered shell element features found in commercially available finite element programs. Historical Guastavino tiles have been tested to obtain material properties. These modern techniques have been employed in conjunction with Guastavino's original empirical design criteria to provide a better understanding of these historically significant structures.

1 Introduction

Rafael Guastavino, born in 1842, emigrated to the United States to establish the Guastavino Fireproof Construction Company. The fascinating architectural legacy of Guastavino and his son (also Rafael Guastavino) has received scholarly attention [1],[2] but the mechanics of his designs have not garnered similar attention from structural engineers. The thin laminated tile construction that the elder Guastavino used in hundreds of structures in the Eastern United States had its roots in his native Catalan's indigenous vaulting tradition. Before emigrating to the United States, Rafael Guastavino designed such laminated vaulting in Barcelona [3]. While it has been suggested that Guastavino came to the United States to utilize superior cements in his mortars [4], others claim it is more feasible to say that he emigrated because of his faith in the American construction industry and its ability to produce consistent and high quality materials [5].

Previous to this study, the engineering material properties of Guastavino tiles have not been quantitatively analyzed, although Lane has performed chemical analyses of the mortars [5]. Much mystery surrounds the formulation of the mortar since many Guastavino vaults were erected without centering or scaffolding. Lane [5] found that many mortars were traditional, simple mixtures of Portland cement and sand, and Parks and Neumann report one part Portland cement to two and one half parts sharp clean sand (specifically Cow Bay sand, a sharp angular sand quarried in Long Island New York [2]). In fact, although Guastavino filed a number of U.S. patents for his fireproof “cohesive” laminated tile construction, none of the patents describe the properties of the mortar, which gives further credence to the theory that the mortar was completely traditional.

Even more mystery surrounds the design methods that Guastavino used in his vaults, arches, domes and stairs. Guastavino claimed that his arches and vaults produced little lateral thrust under gravity loading, and he produced very few design formula in his largely promotional book “Cohesive Construction” [6]. Throughout the history of the Guastavino Company, there appears to have been only one engineer responsible for all design calculations, and his records were lost after the closing of the company in 1962. During the early 1900’s, structural engineers were just beginning to understand the mechanics of thin shell structures, and theories were available only for simple geometries such as hemispheres in the 1930’s. Guastavino combined intuition with empiricism to design spectacular spaces of extreme thinness, doing so with common materials. This paper will analyze some typical designs by means of the finite element method.

2 Mechanical testing of tiles

2.1 Description of recovered tiles

A total of fifteen Guastavino tile fragments were obtained, ranging in size from about 5160 mm², up to 29030 mm², each with a nominal thickness of 2.54 mm. As shown in Figure 1, the tiles were not all the same. In particular, there appeared to be three different groove patterns manufactured in the tiles’ surfaces, varying from small (165 grooves per meter) to medium (138 grooves per meter) to large (106 grooves per meter) grooves. Hence, the first objective of the mechanical testing program was to determine if there were significant differences in mechanical properties, from tile to tile.

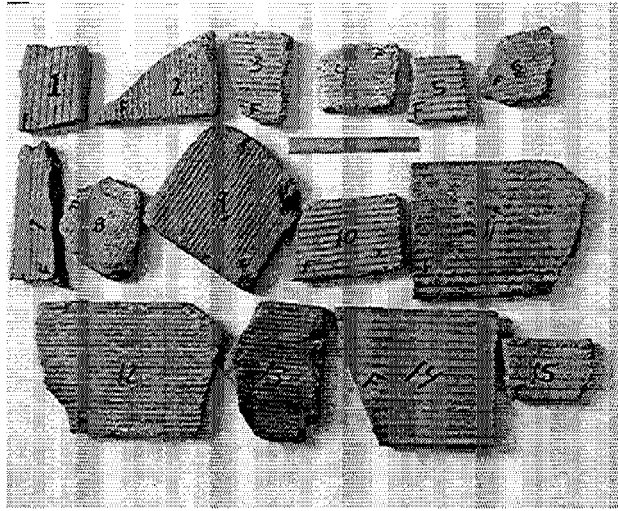


Figure 1: Recovered Tile Specimens.

2.2 Samples and testing

A total of five tiles were tested. Due to the small amount of available tile specimens, it was decided that greatest use would be made from non-destructive testing, which generally requires smaller specimen sizes.

Each of the tested tiles was ground smooth using a diamond abrasive wheel. Then, a water-cooled tile saw was used to cut mechanical testing samples from each tile fragment. Samples were cut in two perpendicular directions, for the purpose of evaluating the anisotropic elastic properties of the tiles. As indicated in Figure 2, the direction of the surface grooves is designated as the X-direction, the direction perpendicular to the grooves is designated as the Y-direction, and the direction through the tile thickness is designated as the Z-direction.

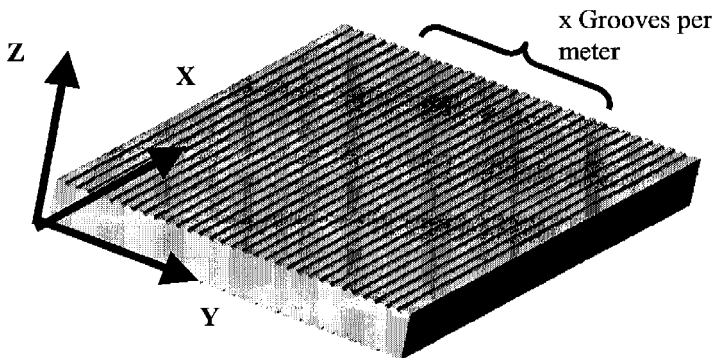


Figure 2: Tile Coordinate System.

2.3 Methods

Mechanical testing consisted of; longitudinal and transverse dynamic elastic modulus testing, monotonic compression testing to determine the ultimate compressive strength, and monotonic flexure testing to determine the ultimate tensile strength.

The longitudinal and transverse dynamic elastic modulus tests were conducted in accordance with ASTM C215 [7], which are free vibration tests, measured via a bonded accelerometer. Data was acquired by a 100 kHz PC-based card, with spectrum analysis provided within the Lab View [8] software package. Typically, the fundamental frequencies of vibration were determined three ways for each sample: the longitudinal (axial) mode, and the transverse (bending) modes, evaluated about both principal bending axes. In every case, the elastic moduli, evaluated three different ways, were in close agreement with one another.

In the monotonic compression tests, a manually-controlled hydraulic testing machine was used to record the ultimate strength of tile samples. For the monotonic flexure testing a manual displacement-controlled testing machine was used to record the ultimate flexural strength of tile samples, in 3-point bending, over spans of 51 mm or 102 mm, where the larger span was used for thicker samples (typically equal to the ground tile thickness of about 20 mm), while the smaller span was used for thinner specimens (typically, 13 mm).

2.4 Mechanical testing results

2.4.1 Dynamic tests for Young's modulus

A total of 38 free vibration tests were conducted on tile samples in the X-direction, while 22 tests were conducted in the Y-direction. For individual tiles, statistical variation was small, with the coefficient of variation for tests within a tile specimen usually less than 10%. This variation tended to be smaller for testing in the X-direction, than in the Y-direction.

The most notable result was consistent orthotropic properties. On average, the dynamic elastic modulus E_x was 21520 MPa in the X-direction, but E_y was only 12000 MPa in the Y-direction. For all tiles, E_x exceeded E_y by a factor of about 1.8. Examining the statistical variation in both directions, it is clear that the orthotropic properties are significant throughout all of the tested tiles. However, despite the presence of orthotropic properties, it is necessary to use an average value for E of about 16548 MPa in structural models, because it is assumed that the tiles were randomly oriented in the structure.

At the onset of testing, it was hypothesized that the differences in surface appearance, namely the sizes of surface grooves, may correlate with differences in properties. Regarding this hypothesis, Table 1 indicates that the tile-to-tile variations are not much larger than the variation of test results within a tile. This suggests that surface appearance does not correlate with X-direction properties.

Similarly, though there are larger tile-to-tile variations in the Y-direction, these variations do not appear to be related to the surface appearance of the tile.

Table 1. Results of dynamic modulus testing.

Tile #	Surface Grooves/m	Avg. E (Mpa)	Number of tests	Coeff. of Variation
X-Direction				
11	106	20154	9	5.3%
14	106	20898	8	8.1%
12	138	25194	9	4.2%
13	165	19133	9	6.5%
8	165	23373	3	7.5%
	<i>Avg X dir.</i>	<i>21520</i>		<i>12.2%</i>
Y-Direction				
11	106	8563	6	4.3%
14	106	13286	4	12.4%
12	138	18340	3	11.4%
13	165	8101	6	9.8%
8	165	18581	3	9.0%
	<i>Avg X dir.</i>	<i>12000</i>		<i>38.3%</i>

2.4.2 Compressive and flexural testing

Due to limits on the available tile specimens, it was not possible to test nearly as many samples destructively, as had been conducted non-destructively. Four compression tests and four flexure tests were conducted, as summarized in Table 2. Although the number of samples does not permit true statistical comparisons, orthotropic properties were, once again, evident. On average, the X-direction compressive and flexural strengths were 34 MPa and 11 MPa, respectively, compared with 23 MPa and 5 MPa in the Y-direction.



Table 2. Experimental tile strength.

Tile #	Surface Groove s/m	Avg. Compr. Strength (MPa)	Number of Compr. tests	Avg. Flex. Strength (MPa)	Number of Flex tests
X-Direction					
11	106	18	1	8	1
14	106	40	1	12	2
12	138	39	2	12	1
13	165	-	0	11	1
8	165	-	0	108	1
	<i>Avg X dir.</i>	34		11	
Y-Direction					
11	106	10	1	3	1
14	106	30	2	6	3
12	138		0	6	1
13	165		0		0
8	165	21	1		0
	<i>Avg X dir.</i>	23		5	

3. Finite element modeling of laminated tile arches

3.1 Finite element input

The commercially available finite element program ANSYS was used to model the tiles and mortar of typical Guastavino arches. An eight-noded isoparametric shell element was used to model both the tile and the mortar. Each element has four corner nodes and four midside nodes, and each node has three translational and three rotational degrees of freedom. The fact that these elements can have layers made up of different material properties was beneficial in modeling the laminated tile structures. To model the structure, rectangular areas were created to match the size of roughly one half of one tile (A1 and A3 in Figure 3). Adjacent to these areas, thinner areas the size of a mortar line were created (A2 and A4 in Figure 3). These areas were meshed as either mortar or tile, so for example, A1, A2 and A3 would be meshed as tile to form one tile unit, then A4 would be meshed as mortar. This pattern was then staggered across the width and through the thickness of the arch. The resulting pattern is stylized in Figure 4.

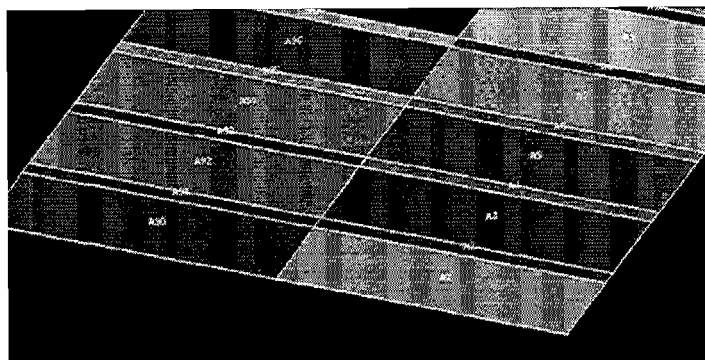


Figure 3: Staggered pattern in finite element model.

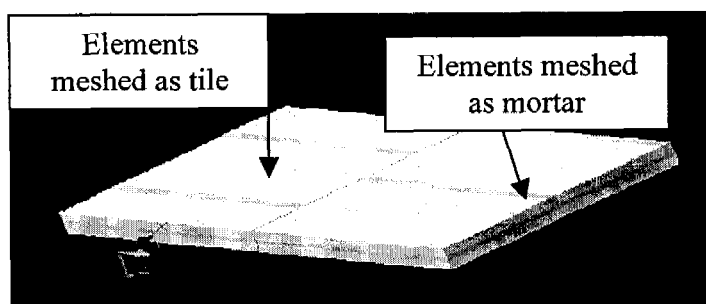


Figure 4: Results of finite element meshing.

Each area was meshed with element sizes of approximately 20 mm width. A representative 0.305 m arch width was modeled, and various span and rise configurations were explored. Three arch spans were studied (1.83 m, 3.66 m and 7.32 m) and for each span, four different rises to the crown were studied (rise 5% of span, rise 10% of span, 15% and 25%). In all arches, the ends were pinned, i.e. fixed against translation but allowed to rotate. This is a conservative assumption.

Tile properties were utilized from the experimental program conducted on the historic Guastavino tiles. As stated before, it was reasonable to assume isotropic material properties for the tile. In this paper, the finite element model used the average isotropic modulus of elasticity $E_{tile}=16458$ MPa and a Poisson's ratio of 0.1. Also studied herein was the effect of varying the mortar modulus of elasticity. The results which follow use a very low modulus mortar,

$$E_{mortar} = \frac{E_{tile}}{32} = 689 \text{ MPa}. \text{ Each arch was modeled as having constant thickness.}$$

The thickness of each arch was prescribed by Guastavino's empirical formula [6] for thickness at the crown of an arch shown in eqn (1).

$$T \cdot C = \frac{L \cdot S}{8 \cdot r} \quad (1)$$

where

- T = thickness at crown of the arch (inches)
- C = compressive strength parameter of tiles (2060 lbf/in²)
- L = loading on arch (lbf / ft²)
- S = span of arch (feet)
- r = rise of arch (feet)

The parameter C (2060 lbf/in² = 14 MPa) is a parameter that Guastavino obtained from testing tiles to failure. It is interesting to note that his failure stress C falls in between the ranges of our failure strengths previously shown in Table 2. A thesis of this paper was that Guastavino's empirical design method shown in eqn (1), which took into account the span, the rise and the loading of a given arch, would have peak compressive stresses at some safe factor below the failure strength C. As seen in Table 3, all peak compressive stresses are at most ¼ the failure stress of 14 MPa. A very interesting outcome seen in Table 3 is that for all twelve configurations, the peak compressive stress is nearly constant. Furthermore the peak vertical deflection of the arch is also consistent from arch to arch. This is demonstrated by dividing the peak vertical deflection of an arch by the crown thickness of the arch. The surprising result is that the answer is practically constant for a wide variety of arch configurations. Thus, Guastavino's empirical method was robust and conservative and extremely simple to use.

Table 3. Results of Finite Element Analyses.

Arch Name	Span (m)	Rise (%)	Thickness at crown (mm)	σ_3 (MPa)	Δ_{Max} (mm)	$(\sigma_3/E)*1000$	$\Delta/thick$
1A	1.83	5	18.5	4.74	1.16	0.29	0.06
1B	1.83	10	9.2	4.68	0.64	0.28	0.07
1C	1.83	15	6.2	4.88	0.44	0.30	0.07
1D	1.83	25	3.7	5.50	0.39*	0.33	0.11*
2A	3.66	5	37.0	4.46	2.28	0.27	0.06
2B	3.66	10	18.5	4.46	1.22	0.27	0.07
2C	3.66	15	12.3	4.73	0.88	0.29	0.07
2D	3.66	25	7.4	5.65	0.60	0.34	0.08
3A	7.32	5	74.0	4.59	4.62	0.28	0.06
3B	7.32	10	37.0	4.40	2.43	0.27	0.07
3C	7.32	15	24.7	4.56	1.76	0.28	0.07
3D	7.32	25	14.8	5.30	1.27	0.32	0.09

* This value is Δ at the crown, which is not Δ_{max} for this particular arch.

The following figure demonstrates the effect of varying the modulus of elasticity of the mortar (E_{mortar}). Here, Arch 2B is investigated, with E_{mortar} varying from 689 MPa (the value used in Table 3), to 16548 MPa (which equals E_{tile}).

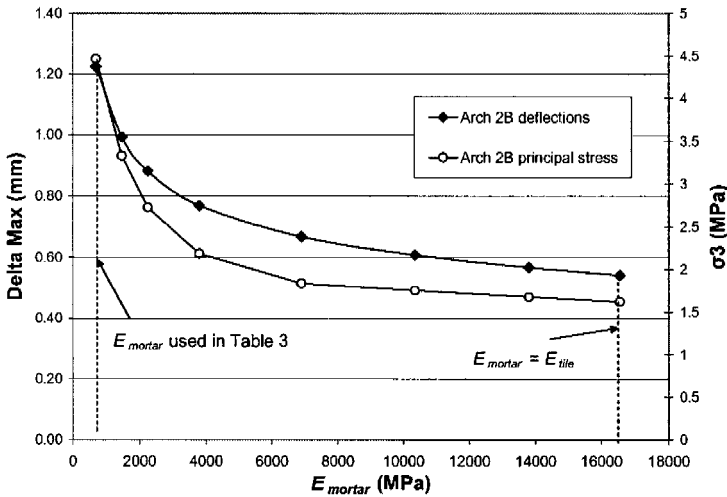


Figure 5: Parametric Study of E_{mortar}

Figure 5 shows that a thirtytwo fold increase in E_{mortar} has a three fold or less effect on peak deflection and principal compressive stress in the arch. This corroborates the previously stated argument that the mortar was traditional and in fact, does not affect the performance of the arches substantially.

4. Conclusions

Guastavino's empirical design method shown in eqn (1) is extremely versatile. By prescribing a thickness for a given arch span, rise and load combination, Guastavino kept the maximum compressive stress a safe factor below the ultimate stress of the tile. Furthermore, the maximum compressive stress obtained for a wide variety of such arches was practically a constant value. The ratio of maximum deflection / arch thickness is also a constant for all the arches investigated herein. The material property testing conducted here was unique and noteworthy, and the values for failure strength correlated very well with Guastavino's published strength values. These material properties, as well as the finite element method described here could be used by other researchers interested in this topic.



References

- [1] Collins, G. The Transfer of Thin Masonry Vaulting. *Society of Architectural Historians*, 27, pp. 176-201, 1968.
- [2] Parks, J. & Neumann, A.G. The Old World Builds the New: The Guastavino Company and the Technology of the Catalan Vault, 1885-1962, Avery Architectural and Fine Arts Library and the Miriam and Ira D. Wallach Art Gallery, Columbia University: New York, pp. 12-51, 1996.
- [3] Neumann, D. The Guastavino System in Context: History and Dissemination of a Revolutionary Vaulting Method. *APT Bulletin*, 30(4), pp. 7-14, 1999.
- [4] Austin, P. Rafael Guastavino's Construction Business in the United States: Beginnings and Development. *APT Bulletin*, 30(4), pp. 15-20, 1999.
- [5] Lane, D. *Putting Guastavino in context: a scientific and historic analysis of this material, method, and technology*. Thesis (M.S.) Columbia University, pp. 33-62, 2001.
- [6] Guastavino, R. Essay on the Theory and History of Cohesive Construction. Thicknor: Boston, pp. 55-149, 1892.
- [7] ASTM C215-97e1 Standard Test Method for Fundamental Transverse, Longitudinal, and Torsional Frequencies of Concrete Specimens, Annual Book of ASTM Standards, Vol. 04.02, 1998.
- [8] LABVIEW Graphical Programming for Instrumentation. Version 4.0. Copyright. National Instruments Corporation, 1995.